

## Structural modification of electrode microstructures in solid oxide fuel cells using high-energy proton irradiation

Young-Sung Yoo<sup>a</sup>, Seung-Muk Bae<sup>b</sup>, Yong-Hoon Kim<sup>b</sup>, Young-Hwan Kim<sup>b</sup> and Jin-Ha Hwang<sup>b,\*</sup>

<sup>a</sup>Green Growth Technology Laboratory, Korea Electric Power Research Institute, 65 Munji-Ro, Yuseong-Gu, Daejeon 305-760, Korea

<sup>b</sup>Department of Materials Science and Engineering, Hongik University, 72-1 Sangsu-dong, Mapo-gu, Seoul 121-791, Korea

**High energy proton beams can be introduced into YSZ/NiO mixtures. In this study, digitized image processing was used to analyze the corresponding microstructure in YSZ/NiO mixtures before and after proton irradiation. High-contrast and high-resolution back-scattered electron images were processed into binary images using a “threshold” function and noise filtering. Quantitative parameters including volume fraction, size distribution, and interconnectivity were estimated. The results indicated that the energetic protons induced a microstructural change in the YSZ/NiO mixtures. Furthermore, the volume fraction and interconnectivity after proton irradiation was increased compared to the initial un-irradiated state.**

**Key words:** Proton Irradiation, Solid Oxide Fuel Cells, Microstructure, Digital Image Processing, Interconnectivity.

### Introduction

Solid oxide fuel cells (SOFCs) have been gaining widespread attention in research and development due to the increasingly high price of fossil-based products and environmental issues attributed to air pollution and global warming [1-5]. The functionality of SOFCs is based on electrochemical reactions at both the cathode and anode, which are separated by solid electrolyte, that occur between 800 and 1000 °C. Electroceramic materials are used for the cathodes and electrolytes in SOFCs. Despite high-temperature operation, the electrochemical performance of SOFCs results in polarization losses at both the cathode and anode. The polarization losses originate from the imbalance between the gas phase, electrons, and ions. Specifically, a reaction between hydrogen, electrons and oxygen ions occurs at the SOFC anode, emitting water vapor. In addition to the electrochemical reaction at the electrolyte/electrodes, the overall performance of the anode is critically dependent on microstructure. Usually, anodic microstructure is determined by the volume fraction, size distribution and interconnectivity of the constituent phases in a mixture comprised of an electrolyte, electronic conductor (i.e., metallic material), and a porous component. In this regard, microstructural control is extremely significant in SOFCs.

Highly-energetic proton irradiation was introduced into solid oxide fuel cells in this study. The high-energy proton irradiation can interact with the anode materials, affecting the electrochemical performance and the corresponding

microstructure. The reducing power of protons can be applied to the anode materials, especially metal oxides that can be reduced to metals, usually under a reducing atmosphere involving hydrogen. YSZ(Y<sub>2</sub>O<sub>3</sub>-doped ZrO<sub>2</sub>)/NiO composites were chosen as a model system to investigate the effect of proton beams on anode materials in SOFCs. Traditionally, electron micrographs have been used qualitatively to understand the structure and processing in a material system under investigation. In this study, the effect of proton irradiation on anodic microstructure was estimated using digitized image processing as a function of the proton dose at a high acceleration voltage (5 MeV). Here, the role of protons in SOFC processing is discussed in the context of large-scale and high-performance SOFCs.

### Experimental Procedure

Green anode substrates (1.0-mm-thick) consisting of nickel oxide (NiO; Sumitomo, Japan) and 8 mol% yttria stabilized zirconia (8YSZ; Tosho Japan) were prepared via thermo-set granulation and uni-axial warm pressing. The ratio of NiO to YSZ was maintained at 56 wt% : 44 wt% in order to control the porous component in the Ni&YSZ anodes after the reduction process. The green NiO/YSZ mixture was sintered to 1,200 °C after complete removal of organic binders at 250 °C. Pre-sintered NiO/YSZ specimens were irradiated in a cyclotron with 10<sup>14</sup> to 10<sup>16</sup> protons/cm<sup>2</sup> at 5 MeV. The proton-irradiated specimens were stored inside a safety storage cabinet until the radioactivity had decreased to ambient levels.

Since the proton-irradiated specimens were highly porous, the porous space of the YSZ/NiO was filled with an epoxy resin. The molded specimens were polished to 0.25 μm using SiC abrasive papers and diamond pastes, depending upon the extent of polishing required. The polished surfaces

\*Corresponding author:

Tel : +82-2-320-3069  
Fax: +82-2-333-0127  
E-mail: jhwang@hongik.ac.kr

were then examined using high resolution field emission scanning electron microscopy (S-4800, Hitachi Ltd., Japan). The microscopy images were collected in two complementary modes, as secondary electron images and back-scattered electron images. The typical acceleration voltage was fixed at 15 keV in both electron microscopy modes. Refined image processing and quantitative analysis was performed using commercial software (Version, Image-Pro, Media Cybernetics, USA). The software was used for capturing the images, image optimization, and data acquisition/analysis.

## Results and Discussion

Electron micrographs are traditionally employed to determine the qualitative features of SOFC electrodes. In this study, electron images were used to quantify microstructural factors in SOFC electrodes including the volume fraction, size distribution, and interconnectivity (or the inverse of tortuosity) [6-9]. This approach included field-emission electron microscopy, which offers the highest contrast and resolution between constituents with the aid of enhanced electron emission from sharp-tipped electron guns. Two-dimensional images can be obtained either in back-scattered electron or in secondary electron modes. Usually, back-scattered electron images provide high contrast due to the higher sensitivity of this mode to the atomic number of the constituents. Fig. 1 shows two typical images of the YSZ/NiO mixtures examined in this study. The back-scattered electron images exhibited higher contrast compared to the corresponding secondary electron images. Accordingly, the BSE images were subjected to subsequent image processing in order to optimize the converted digitized images. The conversion process incorporates image capturing, scale calibration and digitized image processing based on a gray scale. A threshold function and noise filtering are required in order to obtain the simplified binary images that are employed for statistical analyses. The processing steps are illustrated in Fig. 2.

After processing, binary images are then available for the constituent phases (i.e., the solid and pore components). The binary images are analyzed using a well-known microstructural tool using a line intercept method with

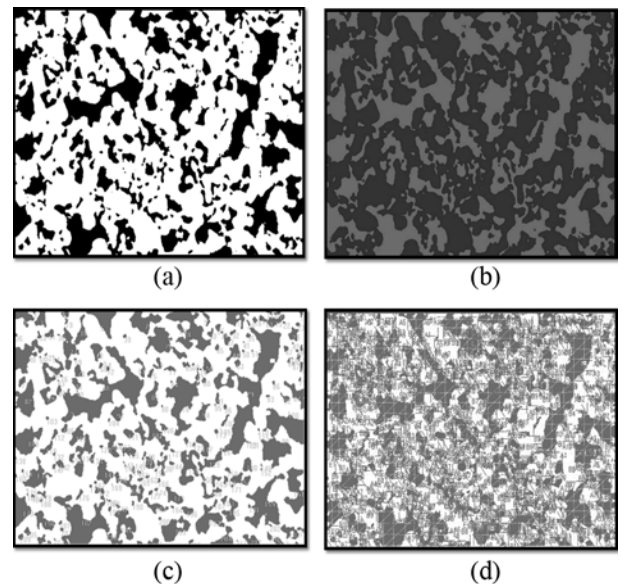


**Fig. 2.** Digital image analysis steps: (a) binary image, (b) deconvoluted image, (c) fraction counting, and (d) the application of line intercepts for statistical analysis.

24 lines in the horizontal direction, 29 in the perpendicular direction and 38 in the diagonal directions. The line segments are statistically processed to determine the average line intercept lengths. Assuming that the microstructure is isotropic in terms of shape and distribution, the volume fraction of the constituent phases is identical to the two-dimensional surface fractions. Based on these fractions and line intercepts, the interconnectivity of the porous and solid components can be calculated based on the following equations:

$$\beta_{Pore} = \frac{V_{Pore}l_{Solid}}{V_{Pore}l_{Solid} + V_{Solid}l_{Pore}} \quad (1)$$

$$\beta_{Solid} = \frac{V_{Solid}l_{Pore}}{V_{Pore}l_{Solid} + V_{Solid}l_{Pore}} \quad (2)$$

Following image analysis for the un-irradiated YSZ/NiO composites, the proton-irradiated YSZ/NiO composites were analyzed in order to quantitatively estimate the microstructural factors. The corresponding two-dimensional BSE images are shown in Fig. 3, along with the digitally-processed binary images. The overall microstructural features of the YSZ/NiO composites are summarized in Table 1.

The volume fraction of the porous component and the corresponding interconnectivity increased with increasing proton dose. This increase in volume fraction and interconnectivity can be attributed to the reducing power and/or heating effect of high-energy protons in porous YSZ/NiO composites. The synergic effect of reducing and heating likely increases the relative fraction of the porous phase and the corresponding interconnectivity. These microstructural changes in porosity and interconnectivity are believed to enhance cell performance especially in terms of mass transport through the porous phase.

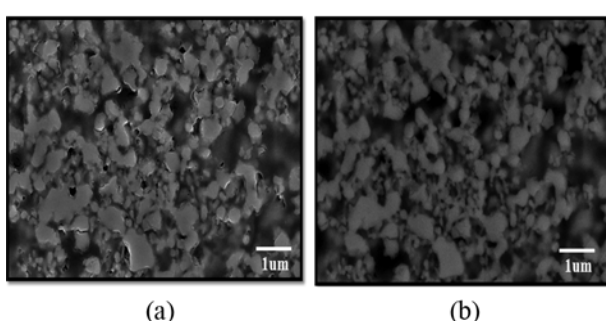


**Fig. 1.** Electron micrographs acquired in (a) back-scattered electron mode and (b) secondary electron mode.

**Table 1.** Summary of the microstructural features of proton-irradiated YSZ/NiO composites

Parameter	Unirradiated Sample	5MeV $10^{14}$ protons/cm <sup>2</sup>	5MeV $10^{15}$ protons/cm <sup>2</sup>	5MeV $10^{16}$ protons/cm <sup>2</sup>
Volume Fraction (Solid Phase)	0.628	0.625	0.54	0.588
Interconnectivity (Solid Phase)	0.725	0.684	0.576	0.62
Average Size [μm] (Solid Phase)	4.037	3.469	5.065	5.809
Volume Fraction (Porous Phase)	0.372	0.375	0.46	0.412
Interconnectivity (Porous Phase)	0.275	0.316	0.424	0.38
Average Size [μm] (Porous Phase)	2.3	2.91	3.603	2.398

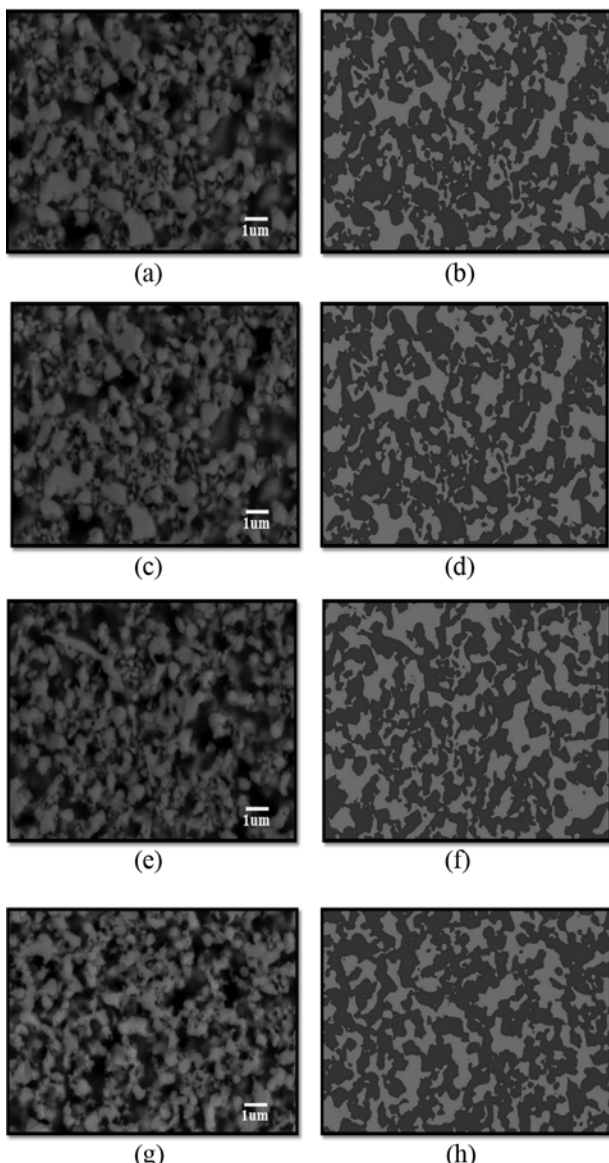


**Fig. 3.** (a), (c), (e), and (f): Original back-scattered electron images. (b), (d), (f), and (h): Digitally phase-separated images before and after proton irradiation used to identify the microstructural changes. (a), (b) : Before proton irradiation; (c), (d) : after proton irradiation ( $10^{14}$  ions/cm<sup>2</sup> and 5 MeV) (e), (f) : After proton irradiation ( $10^{15}$  ions/cm<sup>2</sup> and 5 MeV) (g), (h) : After proton irradiation ( $10^{16}$  ions/cm<sup>2</sup> and 5 MeV)

## Conclusions

Proton irradiation was applied to YSZ/NiO composite anodes. The corresponding microstructural changes were monitored using digitized microscopical processing. The high-energy proton beams appeared to induce microstructural changes in the YSZ/NiO mixtures. The higher the proton dose injected, the higher the volume fraction and interconnectivity of the porous phase. Sophisticated control of the proton dose can be used to dictate the output performance of solid oxide fuel cells.

## Acknowledgments

This research was supported by Basic Research Program in Science and Engineering in Nuclear Applications funded by the Ministry of Education, Science, and Technology, and by a grant from the Fundamental R&D Program for Core Technology of Materials funded by the Ministry of Knowledge Economy, and Korea Electric Power Corporation, Republic of Korea. This was carried out using MC-50 cyclotron at KIRAMS (Korea Institute of Radiological and Medical Sciences). The authors are grateful to J. Y. Han and T. G. Yang for the proton irradiation at KIRAMS.

## References

1. B.C.H. Steele and A. Heinzel, Nature, 414 (2001) 345-52.
2. J.M. Ralph, A.C. Schoeler and M. Krumpelt, J. Mat. Sci., 36 (2001) 1161-72.
3. N.Q. Minh, J. Am. Ceram. Soc., 76[3] (1993) 563-588.
4. S. Tao and J.T.S. Irvine, The Chemical Record, 4 (2004) 83-85.
5. E. Doshi, Von. L. Richards, J.D. Carter, X. Wang and M. Krumpelt, J. Electrochem. Soc., 146[4] (1999) 1273-1278.
6. D. Simwonis, F. Tietz and H. Tagawa, Solid State Ionics, 132 (2000) 241-251.
7. K.B. Alexander, P.F. Becher, S.B. Waters and A. Bleier, J. Am. Ceram. Soc., 77[4] (1994) 939-946.
8. C.S. Smith and L. Guttman, Trans. Metall. Soc. AIME, 197 (1953) 81-87.
9. J.W. Cahn and J.E. Hilliard, Trans. Metall. Soc AIME, 215 (1959) 759-761.